Appendix
Supplementary Material for:

When Yeast Cells Change their Mind: Cell Cycle "Start" is Reversible under Starvation

Deniz Irvali, Fabian P. Schlottmann, Prathibha Muralidhara, Iliya Nadelson, Katja Kleemann, N. Ezgi Wood, Andreas Doncic, and Jennifer C. Ewald

Table of content **page**

Appendix Table S1: Yeast strains used in this study. All strains are W303 derivatives. All strains can be obtained from the corresponding author upon request.

Name	Figures	Genotype	Source
FS042	Non-fluorescent control	MAT a, ADE2, TRP1, LEU2, URA3, HIS3	This study
DI002	Figure 1B,C Figure 2E,F Figure 3 Figure 4D-F Figure 5 A Figure EV1 Movie EV2 App. Figure S3 App. Figure S4 App. Figure S5 App. Figure S6	MAT a, Htb2-mTFP-Nat, Whi5-mCherry-KanMX, Sic1-mNeongreen-hph, ADE2, LEU2, HIS3, TRP1, URA3	This Study
DI028	Figure 1C Figure 2E Figure 3A,B,C Figure 4A-C App. Figure S2 App. Figure S7	MAT a, Whi5-mCherry-KanMX, ura3::Cln2-promoter-mNeongreen-URA3, ADE2, TRP1, LEU2,	This Study
FS034	Figure 2 Movie EV1 App. Figure S2	MAT a, Whi5-mCherry-KanMX, leu2::cln2-promoter-dPSTR-mCitrine-LEU2, ADE2, TRP1, URA3	Ewald Lab [1]
FS002	Figure 1C Figure 2E Figure 3C-D Figure 5 A-B App. Figure S11	MAT a, Whi5-mCherry-KanMX, Sic1-mNeongreen-hph ADE2, TRP1, LEU2, URA3, HIS3	This study
KCY003		mat α, whi5Δ::CglaTRP11, ADE2	Kind gift of Kora-Lee Claude and Kurt Schmoller
DI011	Figure EV2	MAT α, whi5::CglaTRP11, ura3::Whi5-wildtype-mNeongreen-URA3, ADE2 LEU2	This Study (from KCY003)
DI041	Figure EV2	MAT α, whi5::CglaTRP11, ura3::Whi5-7A*-mNeongreen-URA3, ADE2 LEU2 *S78, S113, S114, S149, S76, T281, S288 mutated to alanine	This Study (from KCY003)
DI031	Figure 5A	MAT a, Whi5-mCherry-KanMX, Cip1::HphMX ADE2, TRP1, LEU2, URA3	This Study
DI045	Figure 5A	MAT α, Whi5-mCherry-KanMX, Msn2::HphMX Msn4::HisMX, ADE2, TRP1, URA3	This Study
BY6883		MAT a, Msa1::HIS3, Msa2::KanMX ADE2, TRP1, LEU2, URA3	Breeden Lab [2]

DI047	Figure 5A	MAT a, Msa1::HIS3, Msa2::KanMX Whi5-mNeongreen-Hph, ADE2, TRP1, LEU2, URA3	This Study (from BY6883)
BY6602		MAT a, Xbp1::KanMX, ADE2, TRP1, LEU2, URA3, HIS3	Breeden Lab [2]
DI043	Figure 5A	MAT a, Whi5-mNeongreen-HphMX, Xbp1::NatMX, ADE2, TRP1, LEU2, URA3, HIS3	This Study (from BY6602)
BY6828		MAT a, Sic1::KanMX, ADE2, LEU2, TRP1, HIS3, URA3	Breeden Lab [2]
DI038	Figure 5A	MAT a, Whi5-mNeongreen-HphMX, Sic1::KanMX ADE2, LEU2, TRP1, HIS3, URA3	This Study (from BY6828)
DI040	Figure 5A	mat a, Whi5-mCherry-KanMX, htb2-TFP-NAT, Rim15:: HphMX, ADE2, TRP1, LEU2, URA3	This Study
JE616	Figure 5A Figure 6 Figure EV3	MAT α, cln1∆, cln2∆, cln3::LEU2, lexOPr-Cln1-Leu2, ADE2, his3::cyc1-Pr-lexO TF-HIS3, TRP1, URA3, Whi5-GFP-NatMX	Ewald Lab [3]
KK079	Figure 6	mat α, cln1Δ, cln2Δ, cln3::LEU2, lexOPr-Cln1-Leu2, ADE2, his3::cyc1-Pr-lexO TF-HIS3, TRP1, URA, Whi5::Whi5-V5-KanMX	This Study
KK083	Figure 6	mat α, cln1Δ, cln2Δ, cln3::LEU2, lexOPr-Cln1-Leu2, ADE2, his3::cyc1-Pr-lexO TF-HIS3, TRP1, URA,Whi5::Whi5-Flag-HphMX	This Study
KK087	App. Figure S10	mat α, ADE2, TRP1, LEU2, his3::LexO transcription factor- HIS3, ura3:: LexA promoter-mKO-URA3(estradiol inducible mKO)	This Study
DI036		mat a, Whi5-mCherry-KanMX, Htb2-mTFP-NatMX, Cdc55::hphMX, ADE2, TRP1, LEU2, URA3	This Study
TS010	Figure EV3	mat a, Whi5-mCherry-KanMX, swe1::KanMX, ADE2, LEU2, HIS3, TRP1	This Study
KK097	App. Figure S12	mat a, Whi5-mCherry-KanMX, Swe1::KanMX, ADE2, LEU2, HIS3, TRP1, Cdc55::NatMX	This Study
TS007	App. Figure S8	mat a, Whi5-mCherry-KanMX, ADE2, TRP1, URA3, HIS3, LEU2, Clb2-Neongreen-NAT	This Study

KK069	Figure EV3	mat α, cln1Δ, cln2Δ, cln3::leu2, lexOPr-Cln1-Leu2, ADE2, his3::cyc1-Pr-lexO TF-his3, TRP, URA, Cdk1::Cdk1-FLAG-HphMX	This Study
TS019	App. Figure S8	mat a, Clb2-Neongreen-NAT, Whi5-mCherry-KanMX, ADE, TRP, LEU, URA, HIS	This Study

Appendix Table S2: Optical filters for microscopy

Filters used for imaging on a Nikon Ti2-E epifluorescence microscope.
All described filters are manufactured by Chroma and purchased from AHF.

Fluorophore	LED Wave-length	Filter Set	Excitation Filter	Dichroic	Emission Filter
mTFP	475 nm	TFP ET Filter Set	ET445/30x	T470lpxr, Di 25 mm x 36 mm	ZET488/10x
Neongreen	513 nm	YFP ET Filter Set	ET500/20x	T515lp, Di 25 mm x 36 mm	ET535/30m
mCitrine	513 nm	YFP ET Filter Set	ET500/20x	T515lp, Di 25 mm x 36 mm	ET535/30m
mCherry	575 nm	CFP/YFP/mCherry/Cy7 QUAD LED ET	Quadband Exciter ET/422-449/496-517/566-588/709-752	Quadband Beamsplitter (89402bs)	Quadband Emitter ET/463-484/ 529-550/ 605-678/ 773-845

Appendix Table S3: Exposure times and intensities.

Fluorophore	Imaged Protein	Intensity	Exposure Time
mTFP	Htb2	10 %	100 ms
mNeongreen	Whi5, Sic1, Cln2-Promoter, Msn2, Clb2	15 % - 30 %	200 ms - 300 ms
mCitrine	Cln2-promoter-dPSTR	30 %	300 ms
mCherry	Whi5	40 % - 60 %	300 ms - 600 ms

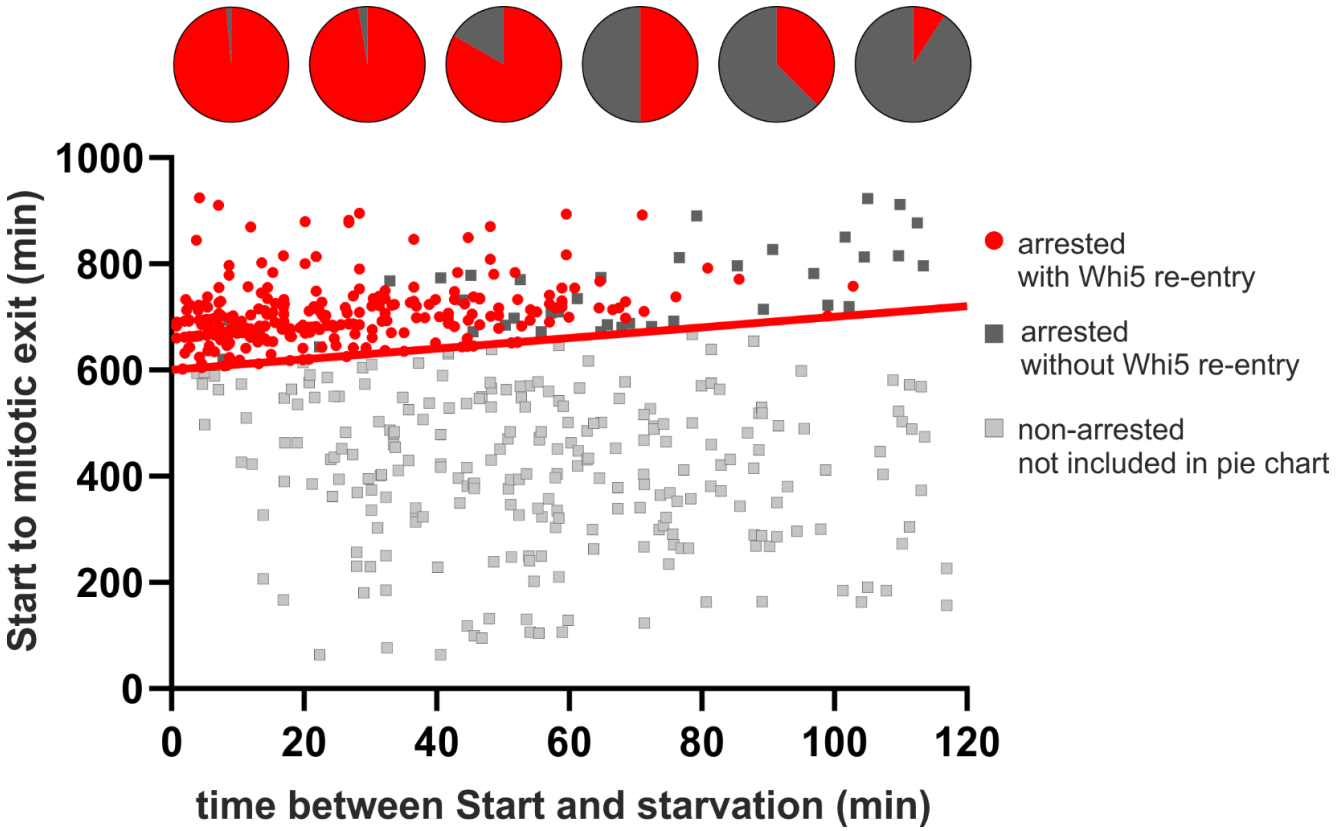

Appendix Figure S1. **Whi5 re-entries**. Same data as in main Figure 1C, but color-coded to show Whi5 re-entries upon starvation. Pie charts show fractions of the arrested cells that re-import Whi5. Pie charts do not include the light-grey non-arrested cells.

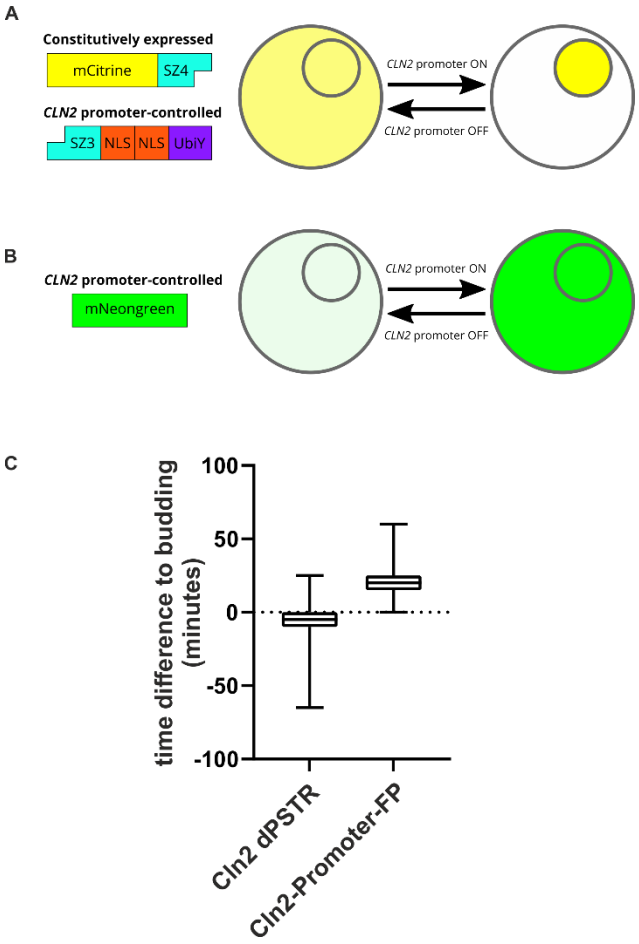

Appendix Figure S2: Cln2 promoter reporters used in this study. The dynamic protein synthesis translocation reporters (dPSTR) developed by the Pelet lab [4] circumvent the time delay in expression analysis caused by fluorescent protein maturation. A fluorescent protein is constitutively expressed, while a small protein containing an interaction domain and a nuclear localization sequence is under control of the promoter of interest. We used this in Figure 2 to monitor the precise timing of Cln2 promoter activation in cells that passed Start before encountering starvation. Since we observed a decrease in total fluorescence during starvation from this construct, we used another construct to monitor Cln2 promoter activity after glucose re-addition. **B.** To monitor Cln2-promoter activity after starvation in Figure 4, we constructed a plasmid containing a Cln2-promoter driving Neongreen expression and integrated it at the URA3 locus. **C.** We analyzed the timing of the peak of the two reporter constructs relative to budding in unperturbed cells. n=231 cells for the dPSTR and n=199 cells for the Cln2-Pr-NG; The box plots indicate the time difference between budding and the peak in the fluorescent signal. Boxes indicate the median and the 25th and 75th percentile, bars indicate 5th and 95th percentile.

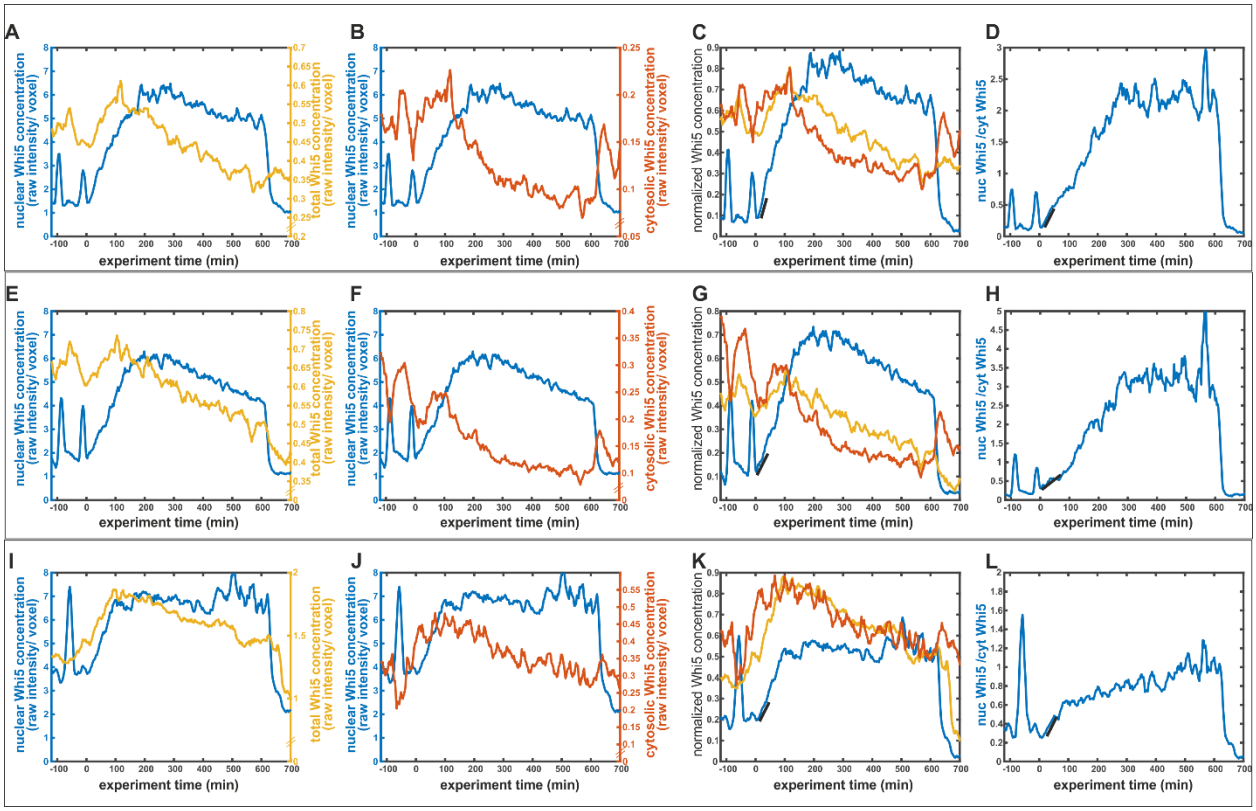

Appendix Figure S3: Whi5 nuclear intensity increase is driven mainly by import-part1. **A.-L.** Here we show three example cells with different Whi5 re-entry slopes, each row represents one cell. Cells were starved between time t=0 minutes and t=600 minutes. We report the raw intensities per voxel (area in pixels$^{3/2}$) for total, nuclear and cytoplasmic Whi5 concentrations (A-B,E-F,I-J). Please note the very different scales in left and right axis. The third plot in each row shows an overlay of the scaled and normalized concentrations (C,G,K). The fourth plot shows the ratio between nuclear and cytoplasmic Whi5 (D,H,L). The black lines in C-D,G-H, K-L indicate schematically the slopes that are plotted in Figure S4. **A-D**. An example cell that was 6 min post Start at starvation onset, was unbudded and had a Whi5- re-entry slope of >200. **E.-H.** An example cell that was 12 min post Start at starvation onset, was still unbudded but had a Whi5- re-entry slope of <200. **I.-L**. An example cell that was 48 min post Start at starvation onset, was budded and had a Whi5- re-entry slope of <200.

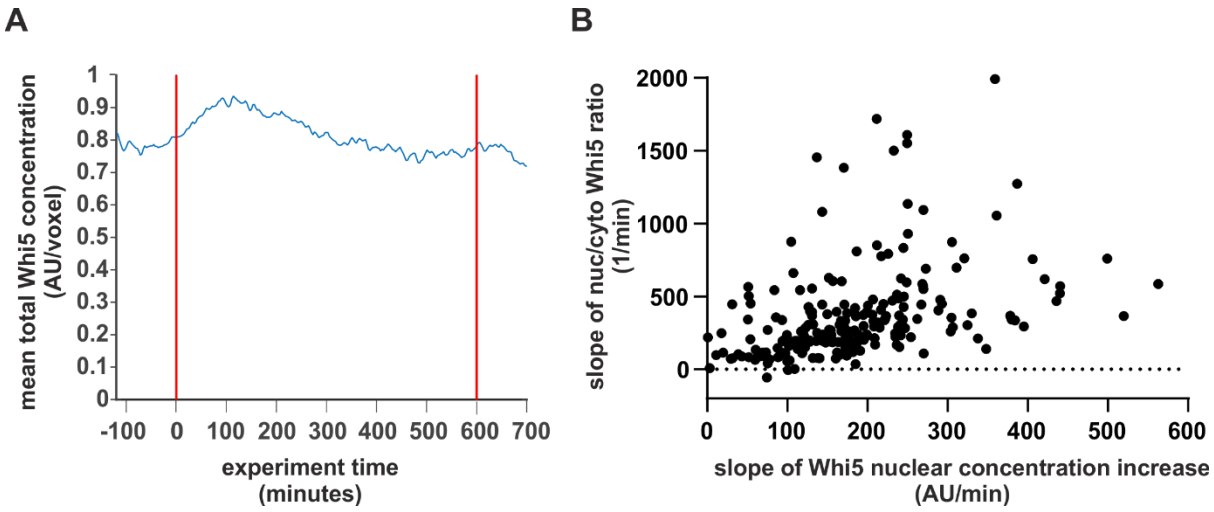

Appendix Figure S4: Whi5 nuclear intensity increase is driven mainly by import-part2 A. Average total Whi5 concentration from 81 asynchronous cells. We cannot disentangle whether the increase is mainly caused by fluorescent artefacts at the onset of starvation or an actual increase in Whi5 transcription. **B.** The slope of nuclear Whi5 concentration (as used in all the main figures) versus the slope of the ratio of nuclear to cytoplasmic Whi5 concentrations (Figure S3 D,H,L) is plotted. (N= 214 cells, data from one replicate each from main Figures 1 and 3.) Since the slopes of the ratios are positive, and the two slopes are correlated, we conclude that the increase in nuclear fluorescence in mainly due to active import, with likely some contribution by an overall increase in Whi5.

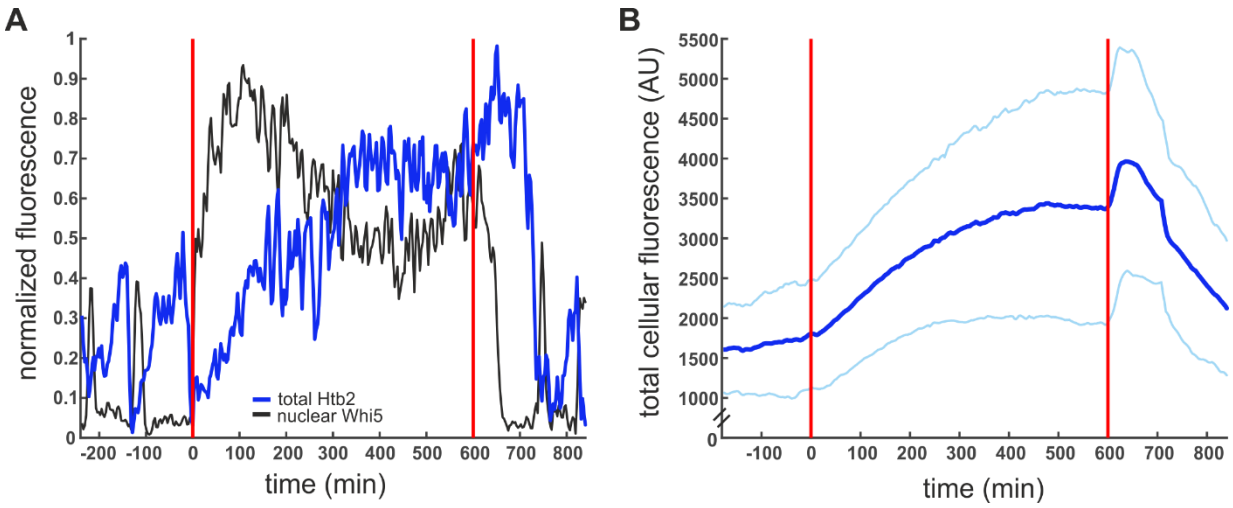

Appendix Figure S5: Starvation induces an increase of Htb2-mTFP fluorescence. **A**. This is an example cell which goes through cytokinesis and enters G1 just before the starvation begins. The black line indicates normalized nuclear Whi5 concentration, the blue line indicates the normalized total cellular Htb2 fluorescence intensity, the red lines indicate beginning and end of the starvation period. Even though the cell is clearly in a normal G1, the Htb2-TFP fluorescence increases more than in a typical pre-starvation S-phase. **B.** Average total Htb2 intensity of 240 asynchronous cells. The light blue lines depict the standard deviation. During starvation, the average fluorescence increases more than twofold, even though only a small fraction of the cells is expected to be in S-phase. Here we plot the total cellular fluorescence; however, the shape of the curve is similar when plotting nuclear total fluorescence or concentration (fluorescence intensity/voxel). A similar effect was observed for Htb2-mCherry.

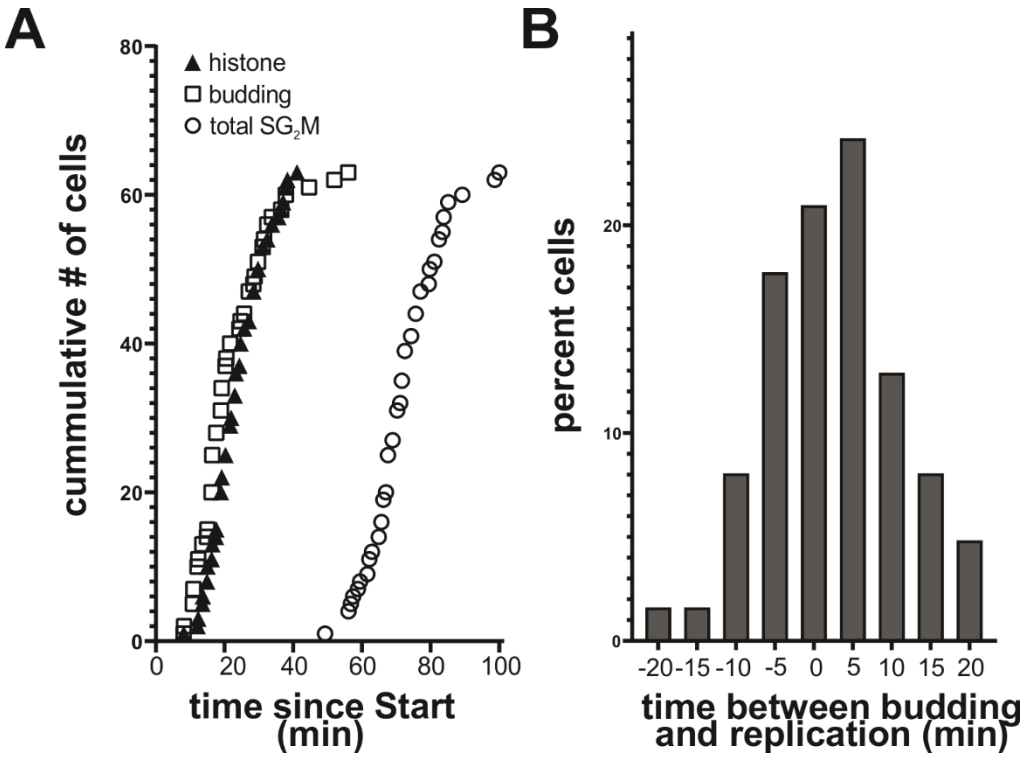

Appendix Figure S6: Budding and replication coincide but are not directly coupled A. Timing of budding and replication in relation to Start of cells growing on glucose minimal medium. Htb2-TFP fluorescence increase was used as a proxy for replication onset. 65 single cells growing on glucose minimal medium were observed and the time between Start, budding, and onset of histone production were recorded. S/G2/M corresponds to the time between Whi5 exit, and Whi5 entry in mother and bud at the end of mitosis. **B.** Histogram of the time difference between budding and increase of Htb2 fluorescence in the 65 cells described in A.

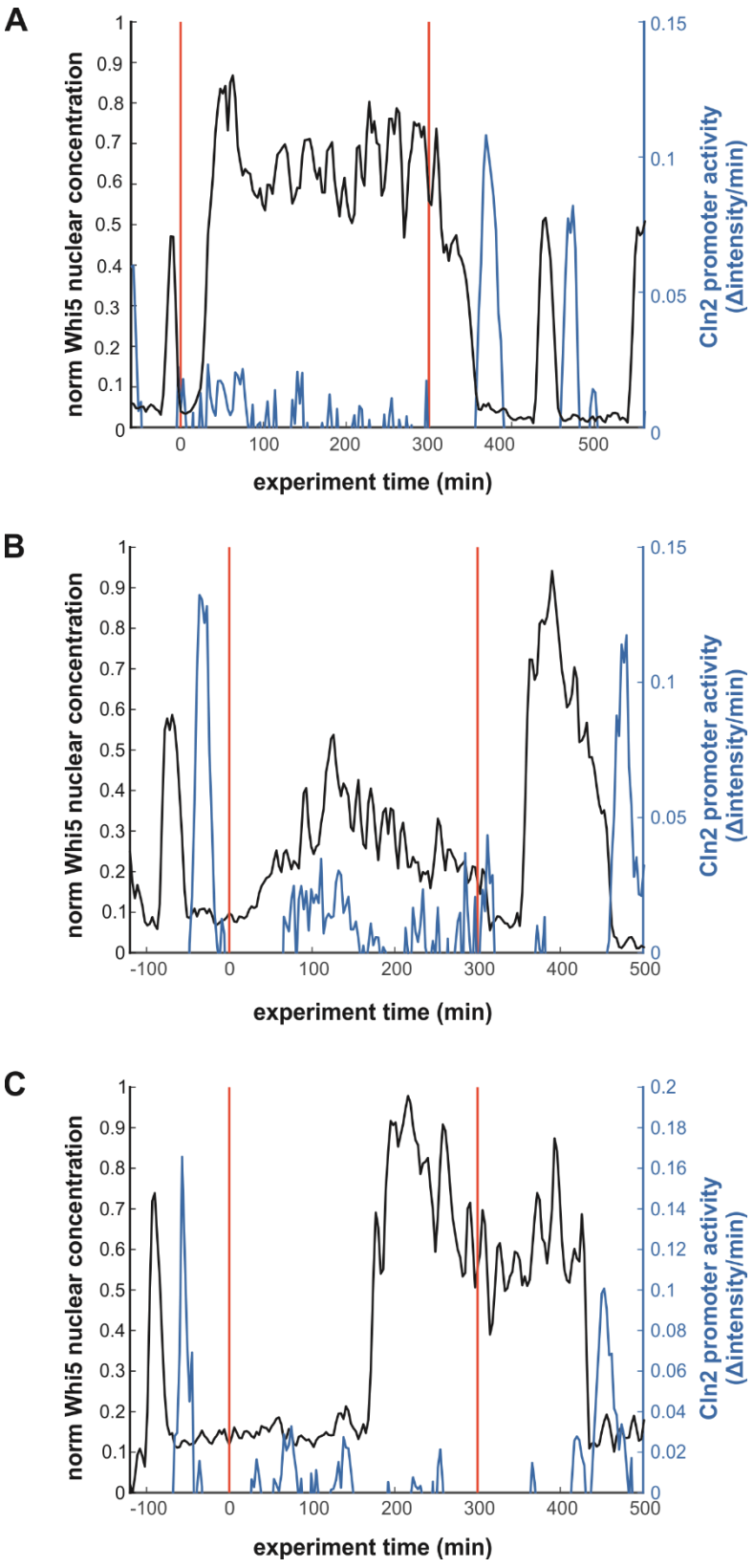

Appendix Figure S7: Examples for Cln2 promoter activity under starvation. Cells were grown on glucose medium, then starved for 5 hours, after which the glucose was replenished. Vertical solid red lines indicate onset and end of starvation phase. **A.** Example of a cell with steep Whi5-re-entry (like Figure 4A). Likely because the time between Start and starvation is too short for the fluorophore to mature, we do not detect the firing of the Cln2 promoter the first time the cell passes Start. However, using the dPSTR construct in Figure 2 we could show that Whi5 exits always lead to Cln2 promoter activity. When glucose is replenished, the Cln2 promoter becomes active again. **B.** Example of a cell with slow Whi5 re-entry. Typically, in cells with slow Whi5 re-entries the initial Cln2 promoter activity can be clearly detected and cells have already passed this peal when Whi5 returns to the nucleus. When glucose is replenished, cells complete their cell cycle without showing a second Cln2 peak. **C**. Example of a cell without Whi5 re-entry ("delayed" category in Figure 1). Cln2 promoter activity can be detected after Start and the cell is already 80 minutes post-Start when faced with starvation. The cell completes the cell cycle and arrests in G1. After glucose replenishment, the cell passes the next Start including Cln2 promoter activity.

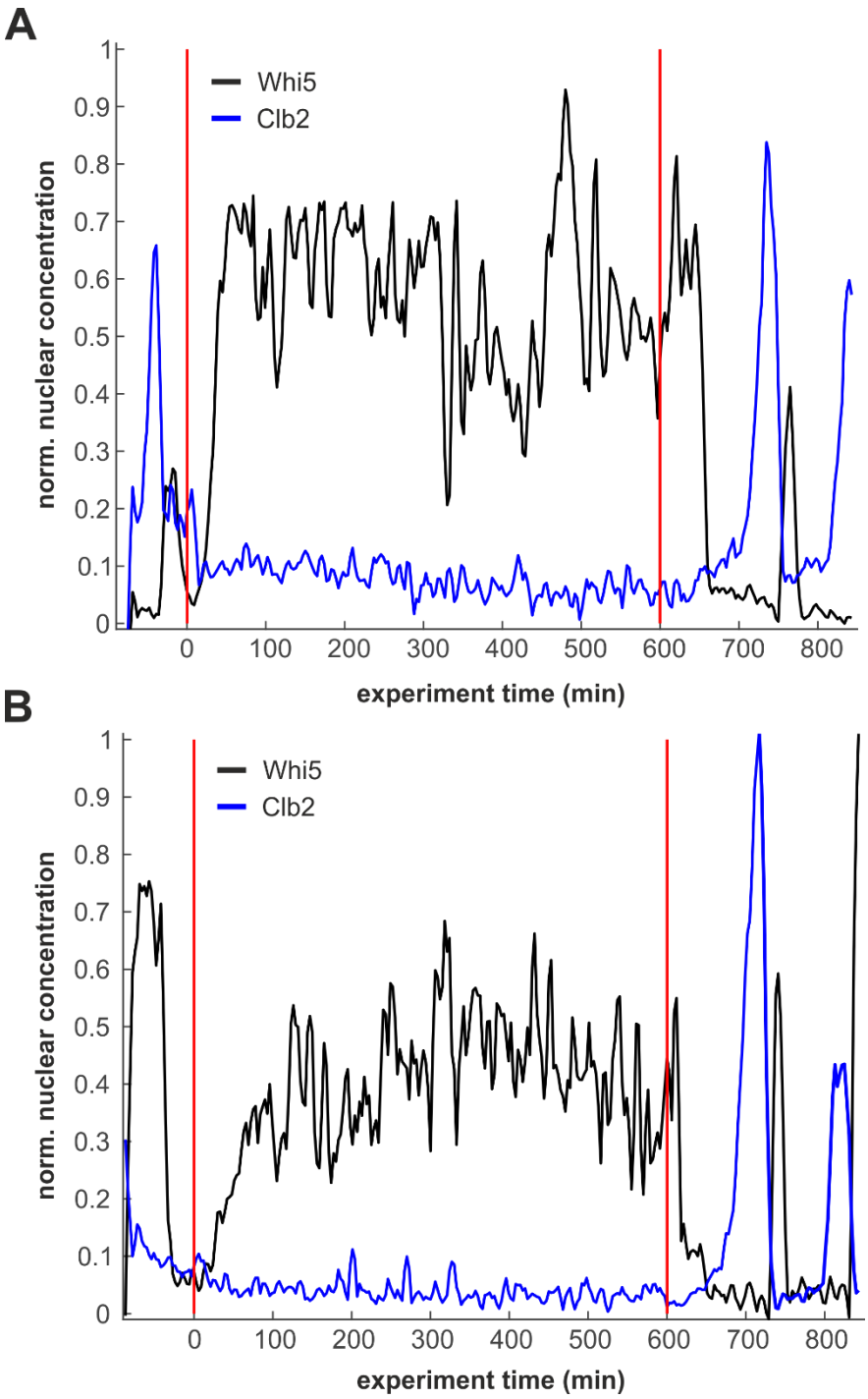

Appendix Figure S8: Expression of Clb2 in Whi5 re-entry cells. Cells expressing Whi5-mCherry and Clb2-Neongreen were grown for six hours on glucose minimal medium and then switched to sorbitol minimal medium at t=0 minutes. All cells in which we could detect Whi5 re-import (n=81, from two biological replicates) displayed a clear peak in Clb2 protein levels (>50% of the last pre-starvation peak) after glucose replenishment and before the next mitosis. This indicates that all cells showing Whi5 re-entry arrest before the G2/M transition. Red lines indicate beginning and end of 10 hour starvation period. **A.** Example cell with a fast Whi5 re-entry (slope >200). **B.** Example cell with a slow Whi5 re-entry (slope <200).

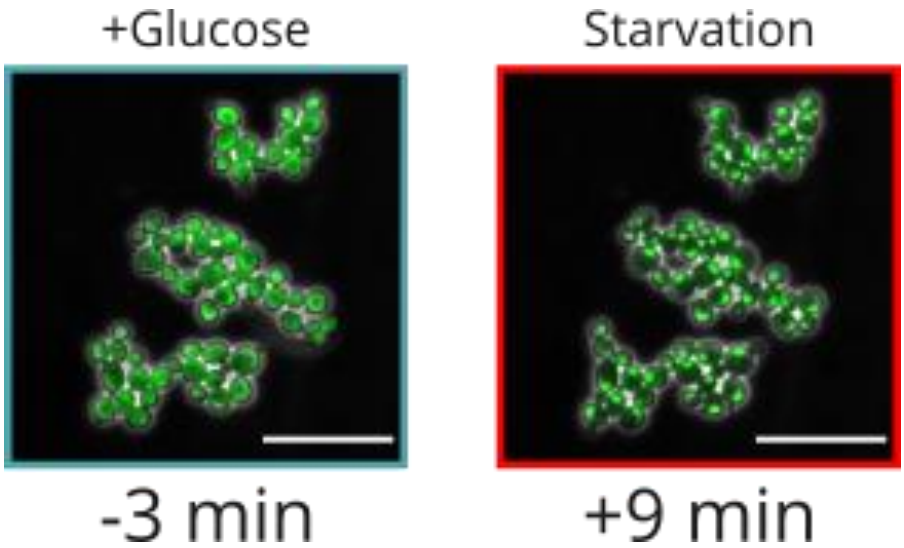

Appendix Figure S9: The response of Msn2 to starvation medium. Cells expressing Msn2-Neongreen were grown for six hours on glucose minimal medium and then switched to sorbitol minimal medium at t=0 minutes. All observed cells imported Msn2 to the nucleus within 10 minutes. The Neongreen signal in both composite pictures was enhanced using ImageJ plug in "Non-Local Means Denoising" [5]. Scale bar represents 20 µm.

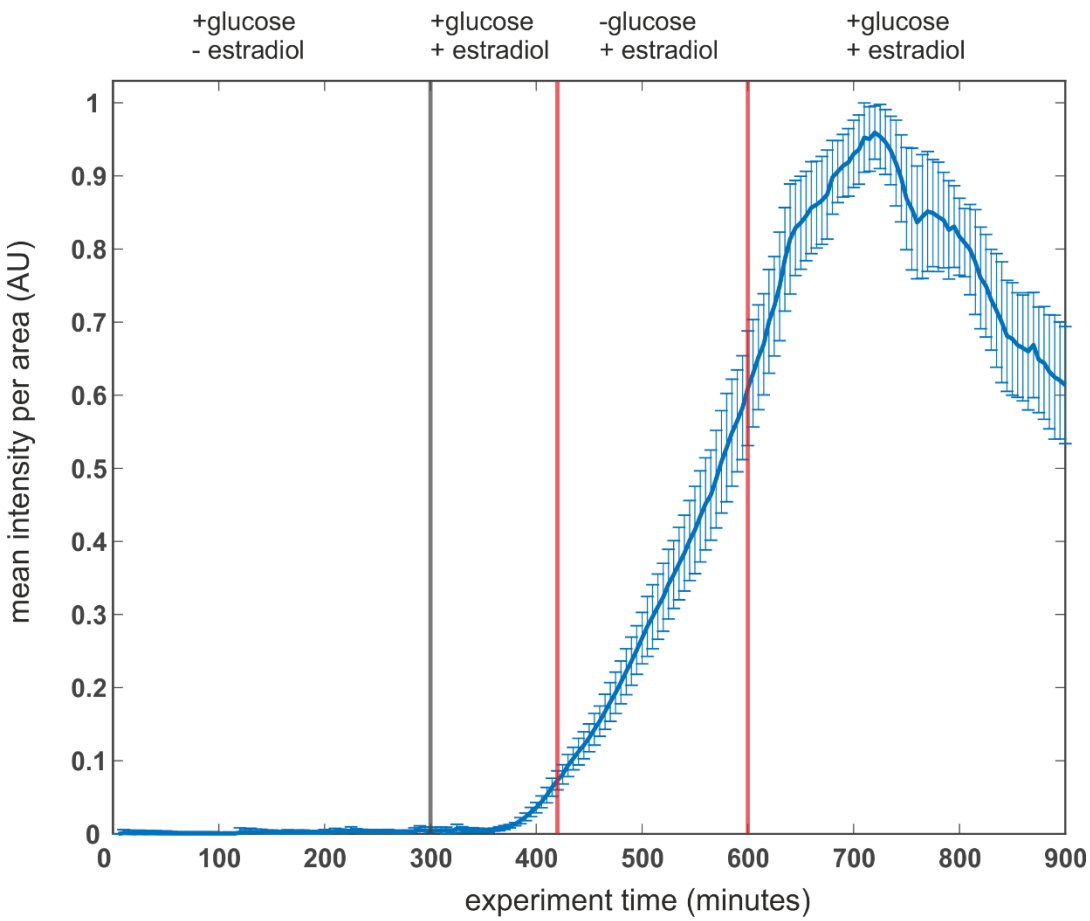

Appendix Figure S10: The estradiol promoter is active under starvation. To test if the estradiol promoter [6] retains activity under starvation, we constructed a plasmid where the estradiol promoter drives expression of the fluorophore mKo. This plasmid was integrated into the ura3 locus. Cells were grown on glucose minimal medium for six hours, when mKo expression was induced by adding 1µM estradiol (the same amount as used for the Cln1 promoter). Two hours later we switched to starvation medium, but maintained the estradiol concentration. Because cells stop growing, but the estradiol promoter is active, cells continuously accumulate fluorescence signal. Shown is the mean and standard deviation of 16 cells.

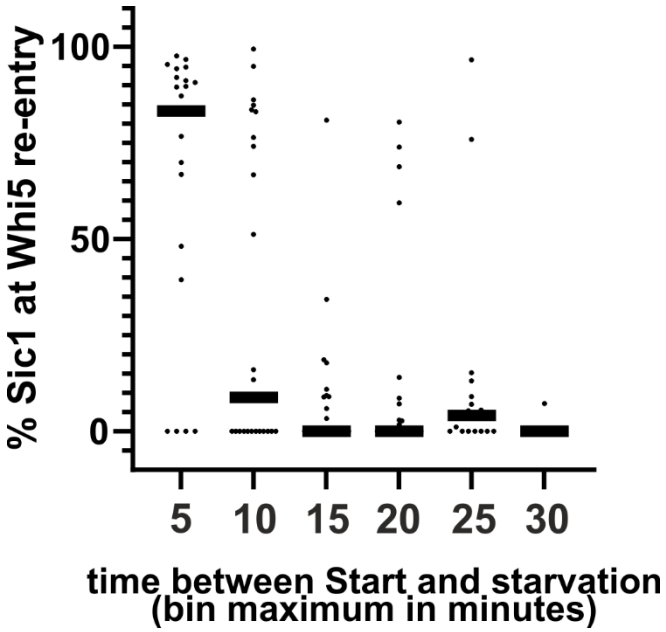

Appendix Figure S11: Whi5 re-entry is independent of Sic1 concentrations. For all cells that showed fast re-entries of Whi5 (i.e. reverse Start), we determined the concentration of Sic1 (total fluorescence per area) at the beginning of Whi5 re-entry. Each dot represents an individual cell (n=149, from two biological replicates), bars represent the bin median.

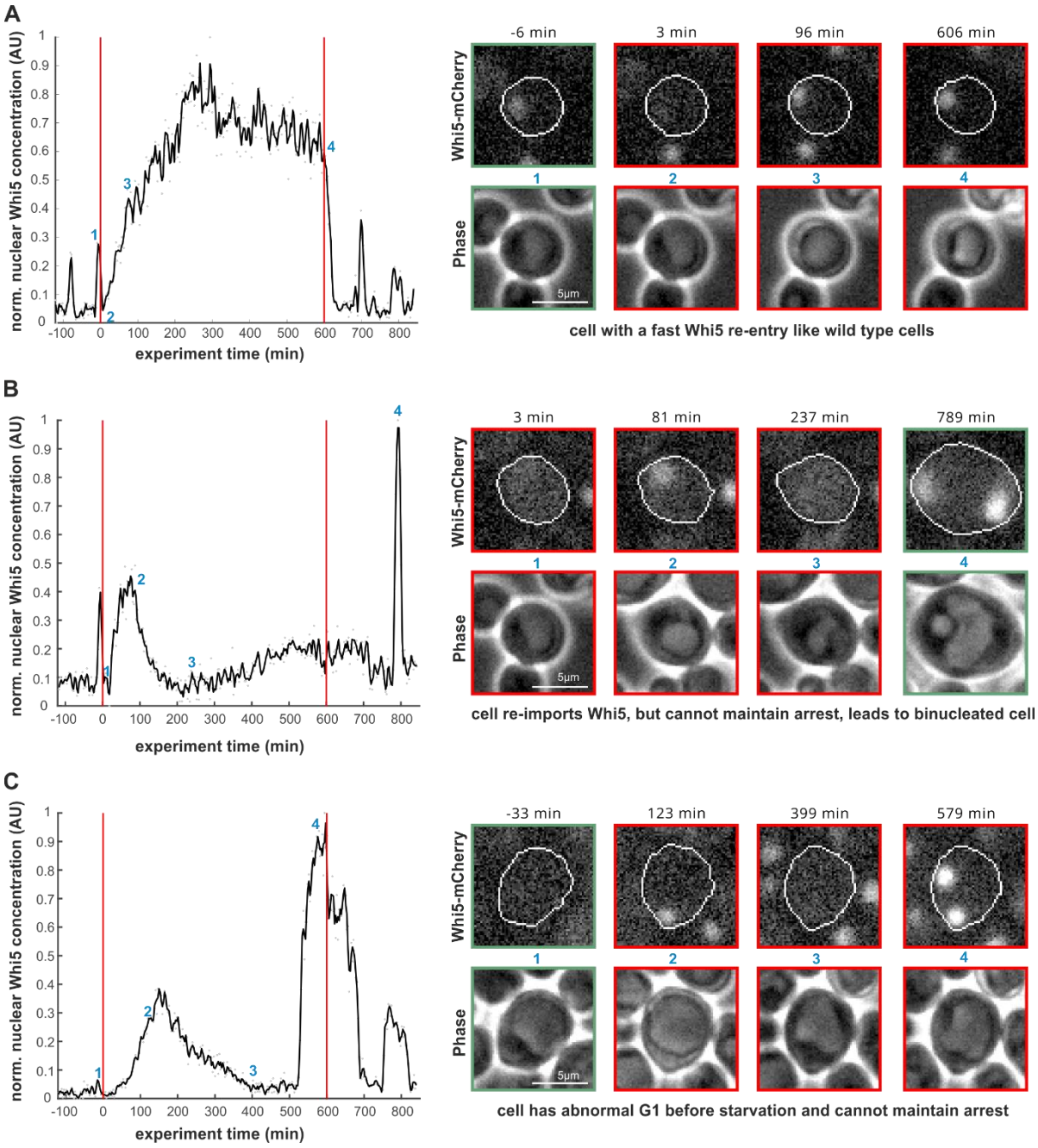

Appendix Figure S12: The phenotype of a *cdc55 swe1* deletion strain. The cdc55 deletion leads to pleiotropic phenotypes that could not be properly analyzed. The *cdc55 swe1* double deletion ameliorates some of the mitotic defects leading to more normal-looking cells. Nonetheless, this double mutant has an irregular G1/S transition and also has difficulties in handling starvation. Three example cells are shown; on the left the quantification of nuclear Whi5, on the right the corresponding images. Blue numbers indicate the time points in the data for which we show the images. Red lines indicate beginning and end of the starvation period. **A.** An example cell that behaves like wild type cells: This cell passes Start approximately 3 minutes before the switch to starvation. It re-imports Whi5 and goes into a stable G1 arrest until glucose is replenished. **B.** An example cell that re-imports Whi5, similar to wild type cells. However, after two hours, the cell cannot maintain this arrest and Whi5 leaves the nucleus. After glucose replenishment, the cell reimports Whi5 into two nuclei, indicating

that there was mitosis without budding, leading to a binucleated cell. A similar phenotype was occasionally also seen in s*we1* single deletion mutants. **C.** This cell, like many *cdc55* mutant cells that we observed, does not show any nuclear Whi5 peak during the very short G1 phases during growth on glucose. Around 35 minutes before starvation the last cytokinesis could be observed, so this cell has likely entered the next round of S-phase when faced with starvation. During starvation, this cell also goes through mitosis without division, leading to a binucleated cell. In summary, our observations suggest that Cdc55 is an important cell cycle regulator during growth and during starvation, but it is not essential for re-importing Whi5 immediately after Start.

Appendix References

1. Nadelson, I., *Sensors for monitoring cell cycle regulation during nutrient perturbations*. 2020, Eberhard Karls University of Tuebingen.
2. Miles, S., et al., *Msa1 and Msa2 Modulate G1-Specific Transcription to Promote G1 Arrest and the Transition to Quiescence in Budding Yeast.* PLoS Genet, 2016. **12**(6): p. e1006088.
3. Ewald, J.C., et al., *The yeast cyclin-dependent kinase routes carbon fluxes to fuel cell cycle progression.* Molecular Cell, 2016.
4. Aymoz, D., et al., *Real-time quantification of protein expression at the single-cell level via dynamic protein synthesis translocation reporters.* Nat Commun, 2016. **7**: p. 11304.
5. Buades, A., Coll, B., Morel, J.-M. , *Non-Local Means Denoising.* Image Processing On Line, 2011. **1**: p. 208–212.
6. Ottoz, D.S., Rudolf, F., and Stelling, J., *Inducible, tightly regulated and growth condition-independent transcription factor in Saccharomyces cerevisiae.* Nucleic Acids Res, 2014.